



OPEN Multiobjective optimal power flow solutions using nondominated sorting colliding bodies optimization

Harish Pulluri¹, Kambhampati Venkata Govardhan Rao², Cholleti Sriram³, B. Srikanth Goud¹, Praveen Kumar Balachandran^{4,5} & Sangeetha K⁶✉

In the current work, an innovative nondominated sorting colliding bodies optimization (NSCBO) technique is introduced to tackle multiobjective optimal power flow (MOOPF) challenges within electrical power networks. This method offers a means to generate a diverse array of nondominated solutions in a single iteration by including the nondominated (ND) sorting process and the concept of crowding distance. Additionally, it utilizes a spread indicator to archive the latest nondominated solutions. In the NSCBO method, the mass of each colliding body is determined by its nondominated rank rather than relying on objective function information. Moreover, a fuzzy decision-making strategy is employed to identify a suitable solution from the set of ND solutions. To showcase the scalability and viability of the NSCBO method, experiments are conducted on IEEE 30-bus, considering both bi- and tri-objective models. Comparative analysis with existing methods from recent literature demonstrates the efficacy of the NSCBO technique in handling constraints and deriving nondominated solutions for MOOPF problems.

Keywords Colliding bodies optimization, Heuristic technique, Objective optimization, Emission pollution, Total production cost

The concept of Optimal Power Flow (OPF) developed by Dommel and Tinney in 1960 holds paramount importance in power system operation and control. The objective of OPF is to identify optimal control variable setups that minimize a selected function while adhering to a series of equality and inequality restrictions¹. Initially, traditional approaches such as linear programming (LP)² and Newton's method³ were employed to address OPF problems. However, these methods face challenges in dealing with nonlinear objective functions and constraints. To overcome these limitations and achieve near-optimal solutions for various optimization challenges^{4–6}, several heuristic techniques have been developed, namely, differential evolution (DE)^{7–10}, genetic algorithm¹¹, particle swarm optimization¹², artificial bee colony (ABC)¹³, harmony search (HS)¹⁴, gravitational search algorithm (GSA)^{15,16}, pathfinder algorithm (PA)¹⁷, imperialist competitive algorithm (ICA)¹⁸, firefly¹⁹, Cascaded fuzzy system^{20,21}, Wavelet-Oriented^{22,23}, stud krill herd²⁴, and machine learning²⁵ methods have been devised to address multiobjective OPF challenges through algorithmic approaches. In⁷ introduced enhanced self-adaptive DE with Mixed Crossover (ESDE-MC) algorithm for MOOPF problems, targeting production costs, emissions, L-index, and power loss minimization. It combines eigenvector and binomial crossovers with adaptive parameter adjustment. Simulation results demonstrate the algorithm's effectiveness for MOOPF problems. In⁸, introduced a multi-objective optimization (MOO) approach for solving the MOOPF problem with improved computational efficiency. By reducing the number of load flows using sensitivities and heuristics, the approach accelerates the solution process while addressing fuel cost, loss, and L index minimization. Tested on the IEEE 30-bus system, it outperforms NSGA-II and can be implemented with various evolutionary algorithms. In¹⁰, the multi-objective adaptive guided differential evolution (MOAGDE) algorithm addressed MOO by enhancing

¹Department of Electrical and Electronics Engineering, Anurag University, Hyderabad 500088, Telangana, India.

²Department of Electrical and Electronics Engineering, St. Martin's Engineering College, Dhulapally, Secunderabad 500100, Telangana, India. ³Department of Electrical and Electronics Engineering, Guru Nanak Institute of Technology, Ibrahimpatnam, Hyderabad 501506, TS, India. ⁴Department of Electrical and Electronics Engineering, Vardhaman College of Engineering, Hyderabad 501218, Telangana, India. ⁵Department of Electrical, Electronic and Systems Engineering, Faculty of Engineering and Built Environment, Universiti Kebangsaan Malaysia, Selangor, Malaysia. ⁶Department of CSE, Kebri Dehar University, Kebri Dehar, Ethiopia. ✉email: sangeethak@kdu.edu.et

exploration and exploitation compared to single-objective algorithms. It utilizes non-dominated sorting and crowding distance for optimal Pareto solutions, validated against the CEC 2020 benchmark suite. Applied to the multi-objective AC optimal power flow (MO-ACOPF) problem with renewable energy sources, the algorithm demonstrated superior performance on the IEEE 30-bus system. In¹¹ presented the Non-dominated Sorting GA II (NSGA-II), which addressed key criticisms of existing MOEAs by offering a fast non-dominated sorting approach with $O(MN^2)$ complexity. It features a selection operator that optimally combines parent and offspring populations and modifies dominance for constrained problems. Simulation results show that NSGA-II achieves superior solution spread and convergence to the true Pareto-optimal front compared to other elitist MOEAs. In¹² proposed a hybrid PSO-Salp swarm optimization (SSO) method for solving the OPF problem, optimizing generation cost, emissions, power loss, and voltage stability. Tested on 18 case studies, the algorithm demonstrates superior performance and robustness. Sensitivity analysis confirms its reliability against parameter variations. In¹³ presented an efficient method for solving the MOOPF problem using ABC algorithm to optimize control variables. It addresses various multi objective functions, including fuel costs, power loss, and emissions, for highly constrained nonlinear optimization. In¹⁴ presented a multi-objective harmony search (MOHS) algorithm for solving the MOOPF problem as a nonlinear constrained multi-objective optimization task. It utilized fast elitist non-dominated sorting and crowding distance techniques to manage the Pareto optimal front, along with a fuzzy mechanism for selecting compromise solutions. The article¹⁵ presented the GSA, inspired by swarm behaviors, for solving MOOPF problems. GSA, based on Newton's laws of gravity and motion, utilizes searcher agents to optimize objectives like fuel cost, active power loss, and voltage deviation. The algorithm is tested on a standard 26-bus system and the IEEE 118-bus system, addressing various combinations of these objectives. Results demonstrate that GSA outperforms other optimization techniques in convergence speed and global search capability. In¹⁶ introduced the non-dominated sorting MO opposition-based GSA (NSMOOGSA) for solving single and MOOPF problems. The algorithm utilizes oppositional learning to enhance population improvement and convergence speed. It effectively manages the Pareto optimal front through non-dominated sorting with crowding distance. Tested on the IEEE 30-bus power system, NSMOOGSA demonstrates significant potential in minimizing conflicting objectives. In¹⁷, presented the MOOPF problem, focusing on generation cost, emissions, real power loss, and voltage deviation while integrating wind, solar, and tidal energy sources. The proposed multi-objective pathfinder algorithm (MOPFA) effectively optimizes these objectives in the IEEE-30 test system, yielding a well-distributed Pareto front and diverse solutions. In¹⁸, introduced the Gaussian Bare-bones MO Imperialist Competitive Algorithm (GBICA) and its Modified version (MGBICA) for optimal electric power planning, focusing on OPF and Optimal Reactive Power Dispatch (ORPD) problems. These problems are formulated as nonlinear constrained multi-objective optimization challenges. Evaluated on IEEE 30-bus and IEEE 57-bus test systems, the proposed algorithms show superior performance compared to existing methods. GBICA and MGBICA effectively address multi-objective electric power planning issues. In¹⁹ presented an improved Firefly Algorithm (IFA) combined with extremal optimization (EO), called IFA-EO, to overcome slow convergence and local optima issues in traditional FA. The method features a hybrid attraction model for better exploration and exploitation, an adaptive step size, and EO for enhanced local search. IFA-EO is tested on three parameter identification problems for photovoltaic models. In²⁰, introduced a dynamic MOO algorithm (DMOA) enhanced by a cascaded fuzzy system (CFS) to improve knowledge transfer and mitigate negative transfer issues in evolutionary transfer optimization (ETO). It adaptively selects previous Pareto solutions and assigns soft labels based on convergence and diversity. The algorithm employs kernel mean matching (KMM) to enhance knowledge transfer efficiency. Extensive evaluations show that CFS-DMOA outperforms state-of-the-art ETO-based DMOAs. In²¹ presents a multi-strategy adaptive selection-based DMOA (MSAS-DMOA) using non-inductive transfer learning for solving DMOPs. It improves knowledge transfer with kernel mean matching (KMM) and avoids conventional labeling. Tested on 14 DMOPs, it shows superior convergence and diversity. Ablation studies validate its ability to mitigate negative transfer. In²² presented HWM2SFLA-PSO, a hybrid meta-heuristic algorithm for solving MOOPF problems with multi-fuel constraints and FACTS devices. It optimizes four objectives: total generation cost, emissions, real power transmission losses, and voltage deviation. Results show HWM2SFLA-PSO's superior performance on IEEE test systems, demonstrating improved execution time and solution quality while avoiding local optima. In²³ presented HRS-DMOA, a dynamic multiobjective optimization algorithm that responds to environmental changes using diversity, memory, and prediction-based strategies.

Colliding Bodies Optimization (CBO), an evolutionary technique developed by Kaveh offers a promising solution for continuous optimization problems²⁶, drawing inspiration from the collision dynamics between two objectives. In CBO, independent variables are analogized as colliding bodies (CBs), where collisions between pairs of CBs lead to enhancements in their positions. Notably, CBO operates without requiring control parameters, making it easily implementable. Its efficacy has been demonstrated across various optimization problems^{27–29}.

However, the conventional CBO method falls short when addressing multiobjective Optimal Power Flow (MOOPF) problems. Addressing this research gap, the authors' contributions: to the current research paper are (i) an extension named nondominated sorting colliding bodies optimization (NSCBO) is proposed to tackle MOOPF problems, (ii) incorporating ND sorting and crowding distance concepts enables the proposed technique to produce a diverse set of ND solutions in a single trial, (iii) each CB's mass is determined by its nondominated rank rather than objective function values, (iv) a spread indicator is utilized to store and update nondominated solutions in an external archive, (v) Using a fuzzy decision method helps in effectively choosing the most appropriate and optimal solution from a set of ND solutions. The scalability and efficiency of the developed NSCBO are validated on IEEE 30-bus, encompassing both bi and tri-objective functions. Furthermore, the obtained results are compared with those of existing techniques documented in contemporary literature.

The main challenges in the current work research are.

1. The conventional CBO technique faces difficulty in multi-objective optimization due to its single fitness value reliance, requiring adjustments to CB mass calculations for multiple conflicting objectives.
2. Ensuring a diverse set of non-dominated solutions can be challenging, necessitating effective crowding distance strategies and efficient archiving to avoid premature convergence.
3. Efficiently updating positions and velocities of colliding bodies while managing a scalable population is crucial, particularly for complex systems like the IEEE 30-bus.

The subsequent sections of the paper follow this structure: Section II outlines the OPF formulation, while Section III elaborates on the NSCBO method proposed to tackle the Multi-Objective Optimal Power Flow (MOOPF) challenge. Section IV exhibits the results obtained across different scenarios, and lastly, Section V encapsulates the conclusions drawn from the study.

Multiobjective optimal power flow formulation

Mathematically, The OPF issue may expressed as below¹²:

$$\min f(x, u) \quad (1)$$

$$\text{to } \begin{cases} g(x, u) = 0 \\ h(x, u) \leq 0 \end{cases} \quad (2)$$

where f indicates an objective; x & u indicates state and independent variables correspondingly. $g(x, u)$ & $h(x, u)$ denote equality and inequality constraints individually.

This study encompasses multiple objective functions, with the formulation of said functions and their associated constraints outlined below⁹:

Objective function models

Optimization of fuel cost (FC)

The fundamental objective function in OPF typically revolves around fuel cost and is expressed below⁹.

$$f_1 = \min \left(\sum_{m=1}^{ng} (a_m + b_m P_{gm} + c_k P_{gm}^2) \right) \quad (3)$$

Where f_1 denotes the minimization of fuel cost; a_m, b_m, c_m indicates the cost coefficients of the m^{th} generator; and P_{gm} indicates the real power of the m^{th} generator.

Minimization of emission profile

The aggregate ton/h of atmospheric pollutants emitted, including sulfur and nitrogen oxides, from fossil fuel-fired units may expressed as below⁹:

$$f_2 = \min \left(\sum_{m=1}^{ng} (\alpha_m + \beta_m P_{gm} + \gamma_m P_{gm}^2 + \mu_m \exp(\xi_m P_{gm})) \right) \quad (4)$$

where f_2 indicates emission released from the thermal power plant; $\alpha_m, \beta_m, \lambda_m, \mu_m, \xi_m$ denotes coefficients of m^{th} the unit, and these values depend on factors such as boiler type, operational parameters, and the type of fuel being utilized.

Minimization of active power loss (APL)

Mathematically, the APL across all transmission lines may expressed as a total active power loss associated with each line and is given below:

$$f_3 = \min \left(\sum_{m=1}^{nl} G_m (V_n^2 + V_o^2 - 2V_n V_o \cos \theta_{no}) \right) \quad (5)$$

Where f_3 symbolizes minimization of APL; G_m represents the conductance of m^{th} the bus; V_n, V_o signifies voltages of n^{th} & o^{th} buses individually.

Constraints

The multiobjective optimization optimal power flow (MOOPF) issue is constrained by a multitude of system requirements, including all the constraints, which may be given below:

Equality constraints

The equality constraints in OPF reflect the fundamental physical principles governing the power system. These constraints are articulated through the following equations:

$$P_{gm} - P_{dm} - V_m \sum_{m=1}^{nb} V_n (G_{mn} \cos \theta_{mn} + B_{mn} \sin \theta_{mn}) = 0 \quad (6)$$

$$Q_{gm} - Q_{dm} - V_m \sum_{n=1}^{nb} V_n (G_{mn} \sin \theta_{mn} - B_{mn} \cos \theta_{mn}) = 0 \tag{7}$$

where $P_{gk}, Q_{gk}, P_{dk}, Q_{dk}$ signifies real and reactive power generations and loads at k^{th} bus respectively; $G_{mn} \& B_{mn}$ indicates the conductance and susceptance among $m^{th} \& n^{th}$ buses individually.

Inequality constraints

The inequality constraints delineate the permissible range for variables, ensuring they remain within feasible limits as given as follows;

$$\begin{cases} P_{gm}^{min} \leq P_{gm} \leq P_{gm}^{max} \\ V_{gm}^{min} \leq V_{gm} \leq V_{gm}^{max} \\ Q_{gm}^{min} \leq Q_{gm} \leq Q_{gm}^{max} \end{cases} \quad m = 1, 2, \dots, ng \tag{8}$$

where, $P_{gm}^{min}, P_{gm}^{max}, V_{gm}^{min}, V_{gm}^{max}, Q_{gm}^{min} \& Q_{gm}^{max}$ signifies low and high values of real power, voltages, and reactive power limits of m^{th} generator respectively, $P_{gm}, V_{gm} \& Q_{gm}$ symbolizes real power, voltage, and reactive power of m^{th} generator respectively.

$$t_m^{min} \leq t_m \leq t_m^{max} \quad m = 1, 2, \dots, nt \tag{9}$$

$$b_{shm}^{min} \leq b_{shm} \leq b_{shm}^{max} \quad m = 1, 2, \dots, nc \tag{10}$$

$$V_{lm}^{min} \leq V_{lm} \leq V_{lm}^{max} \quad m = 1, 2, \dots, nl \tag{11}$$

$$S_{lm} \leq S_{lm}^{max} \quad m = 1, 2, \dots, ntl \tag{12}$$

where $t_m^{low}, t_m^{high}, t_m$ symbolize low and high, transformer tap at m^{th} transformer respectively; $b_{shm}^{low}, b_{shm}^{high}, b_{shm}$, signifies the low, high, and susceptance value m^{th} shunt capacitor respectively; $V_{lm}^{low}, V_{lm}^{high}, V_{lm}$, symbolizes low, high, and voltages at m^{th} load bus respectively; S_{lm}, S_{lm}^{high} denotes MVA flow and high MVA of m^{th} line.

**Non-dominated sorting colliding bodies optimization
Multiobjective optimization**

Multiobjective optimization problems involve the concurrent minimization of multiple objective functions while adhering to a set of constraints.

$$\min F(x, u) = [f_1(x, u), \dots, f_i(x, u), \dots, f_L(x, u)]^T \tag{13}$$

$$s.t \begin{cases} g_m(x, u) = 0 & m = 1, 2, \dots, M \\ h_n(x, u) \leq 0 & n = 1, 2, \dots, N \end{cases} \tag{14}$$

where M, N, O indicate the count of objective functions, equality, and inequalities individually; The

Overview of colliding bodies optimization

Drawing inspiration from the interactions between objects in collision scenarios, Kaveh and Mahdavi introduced a novel evolutionary technique termed CBO in 2014¹⁶. In CBO, the solution set of an optimization problem is metaphorically depicted as a colliding body characterized by specific mass and velocity. The efficacy of a solution is assessed based on its mass value and is calculated as follows:

$$m_g = \frac{1/F(g)}{\sum_{h=1}^{NCB} 1/F(h)} \tag{15}$$

where $m_g \& F(g)$ denotes mass and fitness of m^{th} CB. After arranging all CBs in ascending order and dividing them into two equal groups, the first half called stationary and the second half called moving groups, before the collision the velocities of the two said groups are expressed below:

$$v_g = 0 \quad g = 1, 2, \dots, \frac{NCB}{2} \tag{16}$$

$$v_g = X_{g-\frac{NCB}{2}} - X_g \quad g = \frac{NCB}{2} + 1, \dots, NCB \tag{17}$$

where X_g denote position of g^{th} CB. When the prompting CBs shadow the constant CBs and collisions happen between pairs of CBs, serving two resolves: (i) to adjust the stationary positions CBs for improved placement, and (ii) refining moving objects position. The CBs velocities later the impact is expressed below:

$$v_g' = \frac{\left(m_{g+\frac{NCB}{2}} + \alpha m_{g+\frac{NCB}{2}} \right) v_{g+\frac{NCB}{2}}}{m_g + m_{g+\frac{NCB}{2}}} \quad g = 1, 2, \dots, \frac{NCB}{2} \tag{18}$$

$$v_g' = \frac{\left(m_g - \alpha m_{g-\frac{NCB}{2}}\right) v_g}{m_g + m_{g-\frac{NCB}{2}}} k = \frac{NCB}{2} + 1, \dots, NCB \quad (19)$$

where v_g & v_g' indicates velocities of g^{th} CB prior and after collision; the coefficient of restitution, denoted by α .

Nondominated sorting colliding bodies optimization (NSCBO)

Here is the concept of NSCBO technique for addressing multiobjective OPF (MOOPF) issues. NSCBO initially adjusts the mass of CB to tackle MOOPF issues. Additionally, it employs an elite archive set to retain nondominated solutions attained during evolution. Ultimately, a fuzzy decision technique is utilized to derive the best compromise solution (BCS) from the archive set. The procedural steps for NSCBO technique to solve MOOPF issues are outlined as follows.

Initialization

In NSCBO, each CB is viewed as a solution that is arbitrarily generated in the initialization process. The entire feasible search space for the NSCBO technique, comprising colliding bodies, is combined and expressed below:

$$X = \begin{bmatrix} P_{g1,2}, \dots, P_{g1,ng}, V_{g1,1}, \dots, V_{g1,ng}, t_{1,1}, \dots, t_{1,nt}, b_{sh1,1}, \dots, b_{sh1,nc} \\ \vdots \\ P_{gm,2}, \dots, P_{gm,ng}, V_{gm,1}, \dots, V_{gm,ng}, t_{m,1}, \dots, t_{m,nt}, b_{shm,1}, \dots, b_{shm,nc} \\ \vdots \\ P_{gN,2}, \dots, P_{gN,ng}, V_{gN,1}, \dots, V_{gN,ng}, t_{N,1}, \dots, t_{N,nt}, b_{shN,1}, \dots, b_{shN,nc} \end{bmatrix} \quad (20)$$

Nondominated sorting process

In the NSCBO framework, the initialization of the CBs population follows Eq. (20). To categorize the CBs into distinct nondomination layers, a procedure for nondominated sorting is outlined as explained below:

- Step 1: Every CB result assesses all objectives and later determines two factors: (i) the domination count n_p , that dominates the given solution p , (ii) a S_p solutions set dominated by the given one. In the initial ND front, all solutions have zero domination count.
- Step 2: Solutions having zero domination count from the initial ND layer, identified as the Pareto optimal front with a rank of 1.
- Step 3: For every solution p with a domination count of zero, examine every q of its dominant sets S_p and decrease their domination counts by one. If any member's domination count reaches '0' in this process, place it in the second nondomination layer and assign it a rank of 2.
- Step 4: Following the same procedure for every CB of the second nondomination layer identifies subsequent nondomination layers. Repeat until all nondomination levels are established.

In selecting superior CBs, preference is given to those with lower ranks. When CBs share the same rank, those with greater crowding distances are retained within the current population. Hence, the NSCBO technique comprehensive search space necessitates the continuation of operations with a total of CBs.

Update an external archive

The Pareto dominance principle governs the updating of the archive set. If a specific CB in the search area is outperformed by any member of the archive, it is excluded from inclusion in the archive. Conversely, if an individual outperforms one or more members of the archive and is added to the archive cluster the outperformed CBs are eliminated. If the external members beat the extreme archive, the most densely populated region is selected for removal and a spread indicator is introduced to regulate the archive length³⁰. Furthermore, the crowding distance procedure is applied to find the ranking of diverse layers, as elaborated as follows.

$$cd_{s,r} = \sqrt{\sum_{m=1}^{MO} (cd_{s,r}^m)^2}; \quad r = 1, 2, \dots, Al; \quad cd_{s,r}^m = fit_{r+1}^m - fit_{r-1}^m \quad (21)$$

$$SI = \sum_{\substack{r=1 \\ r \neq E_p}}^{Al} |cd_{s,r} - \overline{cd}_s| / (Al - MO) \times \overline{cd}_s \quad (22)$$

where $cd_{s,r}$ denotes crowding distance, MO expresses total number of objectives, Al is the elite external archive length, fit_{r+1}^m , fit_{r-1}^m are the m^{th} fitness of $(r+1)^{th}$ & $(r-1)^{th}$ points. SI indicates the spread indicator.

The definition of CB mass

Based on the literature, it is evident that the classical CBO technique is not suited for addressing MOOPF problems. This limitation arises from Eq. (15), where the mass of each colliding body (CB) signifies the fitness value of a single objective. However, MOOPF problems entail multiple objectives, necessitating a modification of CB masses to accommodate these conflicting objectives. The complexity of calculating mass for multiple objectives lies in the need to consider various fitness values simultaneously, which can introduce challenges in

terms of normalization and aggregation. Specifically, each objective may have different scales and units, making direct comparisons difficult. To address this, the fitness values of all objectives must be normalized, requiring additional calculations to establish a common scale. Once normalized, these values are aggregated to determine the mass of each body, which adds further complexity to the process, as it involves finding a suitable method for combining the normalized values in a way that accurately reflects the trade-offs between the conflicting objectives. This aggregation process must be carefully designed to ensure that the resulting mass representation effectively captures the nuances of the multiobjective optimization problem, as outlined in³⁰.

$$M_g = \sum_{h=1}^M (m_g^h)^2 / \sum_{u=1}^N \sum_{v=1}^M (m_v^u)^2 \tag{23}$$

$$m_v^u = \frac{F_v^u - worst^u}{best^u - worst^u} \quad u = 1, 2, \dots, M \tag{24}$$

where M_g shows mass of g^{th} CB; m_v^u denotes normalized fitness value; $worst^u, best^u$ indicate represent worst and best fitness values in all the CBs of u^{th} objective.

Update positions of CBs with changed velocities

As a result of the updated velocities, all the CBs are adjusted as follows:

$$X_m^{J+1} = X_m^J + rand(1, NCV) * V_m^J \quad m = 1, 2, \dots, \frac{NCB}{2} \tag{25}$$

$$X_m^{J+1} = X_{m-\frac{NP}{2}}^J + rand(1, NCV) * V_m^J \quad m = \frac{NP}{2} + 1, \dots, NCB \tag{26}$$

where X_m^{J+1}, X_m^J indicate positions of m^{th} CB in $(m + 1)^{th}$ & m^{th} iterations; and NCV denotes number of control variables.

Elite archive updating procedure

The upcoming generation's CBs comprise the edge points of optimal solutions within the external archive, strategically positioned in the least congested region. As proposed in³⁰, preserving elite CBs enhances performance and safeguards against losing valuable solutions. Consequently, a random selection of the percentage of CBs from the archive is incorporated into the CBs list. Subsequently, the total number of bodies is capped by eliminating the poorest colliding bodies, commencing from the preceding layer of the ND sporting bodies.

Fuzzy decision-making technique

In MOO with Pareto front issues, the objective is to identify solutions that are not dominated. In such problems, a solution is considered nondominated if improving one objective function can only be achieved by compromising another. Methodologies employed to tackle these problems vary in two key aspects: (i) the approach to generating the nondominated solution set, and (ii) the method of engagement with decision-makers, including the type of information provided such as trade-offs. Selecting the BCS from the trade-offs is crucial in the decision-making procedure. To end, a fuzzy decision procedure is utilized to attain an appropriate and optimal compromise solution from the non-dominated set. The determination of the membership function $\mu(f_p)$ is done independently by taking into account the lower and higher values of each objective, as well as the rate at which satisfaction increases as specified in³⁰.

$$\mu(f_p) = \begin{cases} 1 & f_p \leq f_p^{min} \\ \frac{f_p^{max} - f_p}{f_p^{max} - f_p^{min}} & f_p^{min} < f_p < f_p^{max} \\ 0 & f_p \geq f_p^{max} \end{cases} \tag{27}$$

The membership function values indicate the degree to which a nondominated solution satisfies the f_p objectives, measured on a scale of 0 to 1. Assessing the sum of membership function values ($\mu(f_p); i = 1, 2, \dots, MO$) across all objective functions allows for the evaluation of each solution's effectiveness in meeting the objectives. The performance of every ND solution can be compared to others by normalizing its values relative to the total sum, as defined below:

$$\mu_D^q = \left[\sum_{p=1}^{MO} \mu(f_p^q) \right] / \left[\sum_{q=1}^{ND} \sum_{p=1}^{MO} \mu(f_p^q) \right] \tag{28}$$

where μ_D^q indicates normalized membership function within a fuzzy set; The solution achieving the highest normalized membership μ_D^q within the fuzzy set $max \{ \mu_D^q; q = 1, 2, \dots, ND \}$ should be selected as the BCS.

Sequential instructions NSCBO technique for multiobjective OPF issues

The computational structure of the proposed NSCBO approach, along with comprehensive procedural guidelines and the flowchart illustrated in Fig. 1, for addressing MOOPF problems, is outlined as follows:

- Step 1. Specify the NSCBO parameters, such as the number of CBs (NCB), archive size (A), and maximum iteration count (I_{max}).
- Step 2. Initialization: Generate each CB, indicating a potential solution of an objective function with CVs randomly generated.
- Step 3. Evaluate the fitness value of each CB is expressed below:

$$|F| = f_j + w_P(|P_{g1} - P_{g1}^{lim}|)^2 + w_V(|V_i - V_i^{lim}|)^2 + w_Q(|Q_g - Q_g^{lim}|)^2 + w_S(|S_l - S_l^{lim}|)^2 \quad (29)$$
- Step 4. Conduct the NS process and save all discovered nondominated CBs X into the archive set, then update it accordingly.
- Step 5. Determine the mass value of each CB. Arrange all CBs as described in Sect. 3.2. Evaluate the velocities of these groups before collision.
- Step 6. After the moving CBs trail the stationary CBs and a collision occurs among them, update the velocities of the CBs post-collision.
- Step 7. If the at-most generation has not been reached, return to Step 3; otherwise, display the ND solution in the external archive.
- Step 8. Utilize the fuzzy approach to extract the BCS from the ND solution set.

Pseudocode for proposed NSCBO algorithm	
1:	Assign the NSCBO parameters, namely NCB, archive set (A), and I_{max}
2:	////////////////////Initialization //////////////////////
3:	for each CB $i=1$ to NCB
4:	Initialize the position x_i and velocity v_i
5:	Calculate the fitness each objective of every CB $F_{-objective}(x_i)$ using Eq. (29)
6:	Update the best CB in "A" non-dominated sorting procedure (see 3.3.2)
7:	Calculate the crowding distance for find the ranking of diverse layers using Eqs. 21 & 22

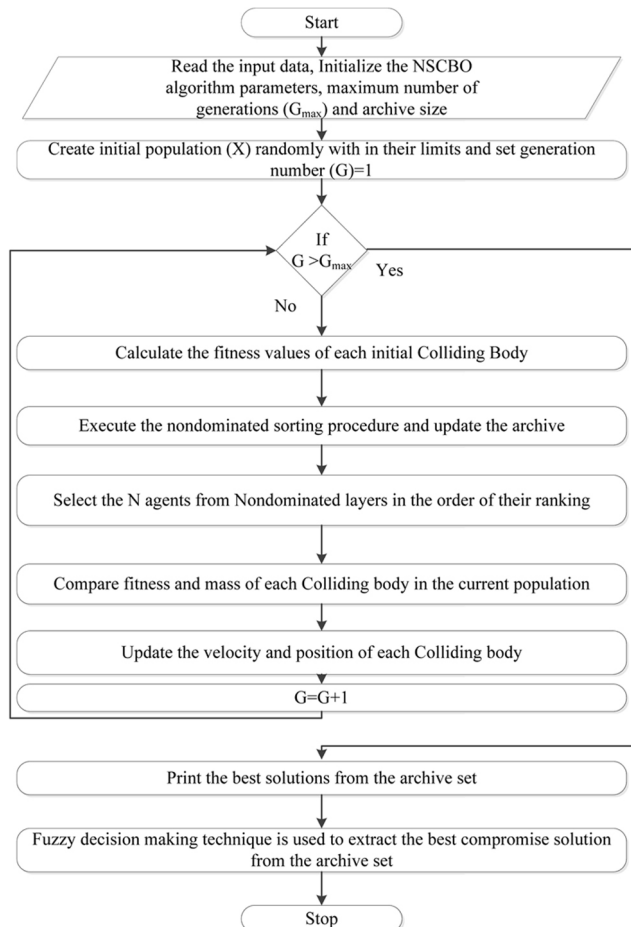


Figure 1. Flowchart of NSCBO approach for MOOPF problems.

Pseudocode for proposed NSCBO algorithm	
8:	end for
9:	While ($k < I_{max}$)
10:	For $i = 1:N_{CB}$
11:	Calculate the Mass of each CB using Eqs. 23 & 24
12:	Update the CB position using 28 & 29
13:	Calculate the fitness each objective of every CB $F_{objective}(x_i)$ using Eq. (29)
14:	Update the best CB in "A" non-dominated sorting procedure (see 3.3.2)
15:	Calculate the crowding distance for find the ranking of diverse layers using Eqs. 21 & 22
16:	End for
17:	Next generation until stopping criteria is satisfied the end while
18:	Find the BCS solution using Eqs. 27 & 28.

Simulation results

To validate and assess the applicability of the developed NSCBO technique, conducted experiments on the IEEE 30-bus featuring two bi-objective issues: namely minimizing TFC & EP, minimizing TFC & APL, and one tri-objective issue involving the optimization of TFC, EP, and APL. The implementation utilized MATLAB 2023a on a PC equipped with a 2.2 GHz i3 core. The parameters for NSCBO included 60 CBs, a maximum of 200 iterations, and an archive set size of 20. Similarly, the reformulated multiobjective differential evolution (MODE) employed 60 chromosomes, a maximum of 200 iterations, an archive size of 20, a mutation rate of 0.6, and a crossover rate of 0.9. The IEEE 30-bus is equipped with 41 lines, 6 generators, 4 transformers, and 9 shunt reactors. It operates with a load of 283.4 MW and involves 24 variables. Voltage and transformer tap settings vary from 0.9 to 1.1 p.u., while shunt reactor values fall between 0 and 0.05 p.u. Bus and line specifications, along with fuel cost coefficients, were obtained from reference¹². To showcase the effectiveness of the NSCBO technique, three distinct scenarios were analyzed.

Case 1: minimization of TFC and EP

Here, the objective is to minimize two conflicting objectives: TFC & EP, treated as a MOOPF issue. Figure 2 illustrates the best set of NDS achieved using the NSCBO technique, indicating its effective exploration of NDS within the search space. Employing a fuzzy decision-making approach, the BCS is determined from all NDS in the archive set. Table 1 presents the best combination of CVs obtained for BCS with both MODE and NSCBO in Case 1, along with corresponding TFC, EP, and APL values. The results achieved with the other algorithms, including NSGA-II¹⁹, VEPSO¹⁹, NEKA¹⁴, Gaussian bare-bones ICA (GBICA)¹⁹, and modified GBICA (MGBICA)¹⁹, as well as MODE, as shown in Table 2. The analysis presented in Table 2 unequivocally showcases that, when contrasted with algorithms documented in existing literature, the NSCBO method consistently outperforms its counterparts by yielding the most optimal values.

Case 2: minimization of TFC and APL

In this context, we tackle the challenge of minimizing TFC while considering APL as an additional objective, forming a MOOPF problem. Figure 3 illustrates the nondominated solutions obtained using the NSCBO method, exposing a diverse collection of Pareto-optimal solutions that are evenly dispersed throughout the search space. Table 1 presents the superior set of control variables, along with corresponding TFC, APL, and EP values attained with both MODE and NSCBO. These results are compared with various algorithms, including

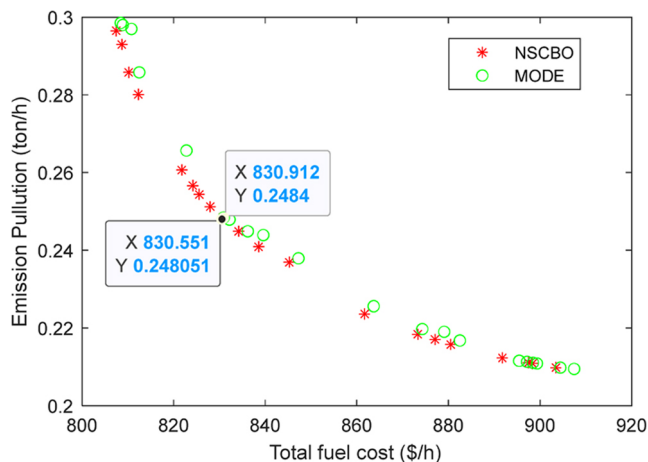


Figure 2. Pareto front attained in Case 1.

Control variables	MODE			NSCBO		
	Case 1	Case 2	Case 3	Case 1	Case 2	Case 3
P_{g1} (MW)	117.6738	122.79	104.248	117.917	122.92	105.10
P_{g2} (MW)	58.3414	52.121	54.7094	56.6998	52.494	58.886
P_{g5} (MW)	27.1461	30.961	30.9903	25.9895	30.998	31.289
P_{g6} (MW)	35.0000	35.000	35.0000	35.0000	35.000	35.000
P_{g11} (MW)	25.7737	26.430	30.0000	27.3524	26.528	29.382
P_{g13} (MW)	25.0592	21.313	33.1979	25.8268	20.681	28.458
V_{g1} (p.u.)	1.0719	1.1000	1.0970	1.1000	1.0999	1.1000
V_{g2} (p.u.)	1.0593	1.0912	1.0777	1.0871	1.0907	1.0847
V_{g5} (p.u.)	1.0323	1.0685	1.0542	1.0555	1.0687	1.0644
V_{g6} (p.u.)	1.0417	1.0781	1.0703	1.0692	1.0775	1.0832
V_{g11} (p.u.)	1.0788	1.0974	1.0941	1.0999	1.0993	1.0895
V_{g13} (p.u.)	1.0501	1.1000	1.0735	1.1000	1.1000	1.0918
t_{6-9} (p.u.)	1.0334	1.0399	1.0050	0.9583	1.0440	0.9722
t_{6-10} (p.u.)	0.9385	0.9243	1.0048	1.0031	0.9000	1.0446
t_{4-12} (p.u.)	0.9796	1.001	0.9844	1.0549	0.9784	1.0151
t_{28-27} (p.u.)	0.9753	0.9774	0.9866	0.9765	0.9652	0.9872
b_{sh10} (p.u.)	0.0126	0.0500	0.0150	0.0388	0.0500	0.0381
b_{sh12} (p.u.)	0.0190	0.0436	0.2379	0.0341	0.0498	0.0124
b_{sh15} (p.u.)	0.0393	0.0461	0.2235	0.0500	0.0471	0.0000
b_{sh17} (p.u.)	0.0488	0.0500	0.4190	0.0001	0.0491	0.0246
b_{sh20} (p.u.)	0.0385	0.0463	0.0366	0.0500	0.0385	0.0376
b_{sh21} (p.u.)	0.0500	0.0500	0.0094	0.0306	0.0500	0.0500
b_{sh23} (p.u.)	0.0257	0.0459	0.0423	0.0000	0.0245	0.0376
b_{sh24} (p.u.)	0.0498	0.0497	0.0325	0.0404	0.0500	0.0376
b_{sh29} (p.u.)	0.0247	0.0217	0.0500	0.0359	0.0233	0.0297
TFC (\$/h)	830.9120	827.791	851.9996	830.551	827.54	847.17
EP (ton/h)	0.2486	0.2603	0.2300	0.2481	0.2540	0.2326
APL (MW)	5.5944	5.2312	4.7459	5.3860	5.2293	4.7238

Table 1. Optimal control variables of BCS were obtained in all cases. Bold Values indicated that the results obtained by the proposed algorithm.

NSGA-II¹⁹, MOHSA¹³, MODE⁹, MOEA/D⁹, and MOABC/D¹², as well as MODE methods, as detailed in Table 2. This analysis underscores the efficiency of the developed NSCBO technique to solve bi-objective issues, demonstrating its capability to generate high-quality solutions across multiple conflicting objectives.

Case 3: minimization of TFC, EP, and APL

Here, addressed a MOOPF issue involving three challenging objectives: TFC, EP, and active APL. Figure 4 displays the nondominated solutions obtained through the NSCBO technique, demonstrating its ability to effectively distribute solutions across a wide range. The optimal set of CVs for this case, with corresponding TFC, EP, & APL values attained with both MODE and NSCBO, are presented in Table 1. Furthermore, Table 2 compared the optimal values of TFC, EP, APL, and execution time (ET) obtained with NSCBO against MODE. These results unequivocally show the superiority of the NSCBO method over MODE. Figure 5 illustrates the high and lower limits of load bus voltages achieved across all three cases, confirming the NSCBO technique's adeptness in handling voltage constraints. Overall, the results substantiate the effectiveness of the proposed NSCBO technique in tackling MOOPF issues, showcasing its capability to generate high-quality solutions and effectively manage conflicting objectives.

Conclusions

In the current research, successfully developed and applied the nondominated sorting colliding bodies optimization (NSCBO) technique for the first time to address multiobjective optimal power flow (MOOPF) issues. The efficacy and reliability of the NSCBO technique were assessed using the IEEE 30-bus system, considering two bi-objectives: minimization of Total Fuel Cost (TFC) and Emission pollution (EP), optimization of TFC and Active Power Loss (APL), as well as one tri-objective involving the optimization of TFC, EP, and APL. The results achieved were compared with other techniques documented in the literature. Based on these comparisons, the developed NSCBO technique consistently yielded feasible and superior optimal solutions across all models when compared to other methods. The key differentiators of NSCBO, such as its unique approach to mass determination based on nondominated rank, normalization of fitness values across multiple objectives, and integration of crowding distance for diversity in solutions, were critical in achieving these outcomes.

Different cases	Method	TFC (\$/h)	EP (ton/h)	APL (MW)	Execution time (ET) (s)
Case 1	MOMICA ¹⁷	865.06	0.22	-	-
	PSO-SSO ¹²	834.80	0.243	-	-
	ESDE ⁷	833.47	0.254	-	-
	NSGA-II ¹⁸	830.8	0.251	-	-
	VEPSO ¹⁸	830.95	0.253	-	-
	MOEA/D-SF ¹⁷	829.515	0.250	-	-
	NKEA ¹⁸	830.85	0.249	-	-
	GBICA ¹⁸	830.85	0.248	-	-
	MGBICA ¹⁸	830.85	0.248	-	-
	MODE	830.9120	0.248	-	54.3
	NSCBO	830.55	0.248	5.3860	47.2
Case 2	MOAGDE ¹⁷	821.839	-	9.9646	-
	MOEA/D-SF ¹⁷	881.01	-	4.144	-
	NSGA-II ¹⁷	837.41	-	5.0397	-
	MOHS ¹⁴	832.67	-	5.3143	-
	DE ⁹	828.59	-	5.69	-
	MOEA/D ¹³	827.71	-	5.2556	-
	PSO-SSO ¹²	865.1	-	4.093	-
	MOABC/D ¹³	827.63	-	5.2451	-
	MODE	827.79	-	5.23	56.3
	NSCBO	827.54	0.254	5.2293	48.2
	Case 3	MODE	852.0118	0.2300	4.7502
NSCBO		847.1749	0.2326	4.7238	63.29

Table 2. Comparison of BCS obtained in different cases with other methods. Bold Values indicated that the results obtained by the proposed algorithm.

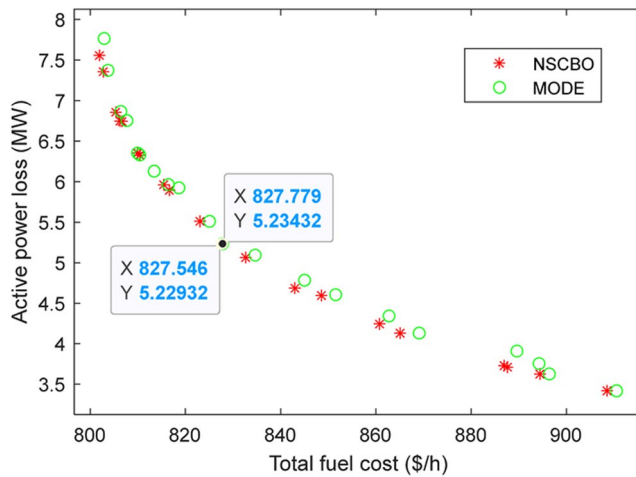


Figure 3. Pareto front attained in Case 2.

Additionally, the incorporation of fuzzy decision-making enhanced the robustness of the solution selection process, allowing for effective handling of uncertainties in the objectives. Therefore, that the NSCBO technique is an efficient and reliable approach to solving MOOPF issues. This study underscores the potential of NSCBO as a valuable tool in the field of power systems optimization, offering improved solutions and contributing to advancements in multiobjective optimization techniques. Given its demonstrated effectiveness, future work may focus on implementing the proposed NSCBO technique to tackle the multiobjective Combined Heat and Power Economic Dispatch (CHPED) problem, especially with the inclusion of renewable energy sources. This expansion of applications not only showcases the versatility of the NSCBO approach but also its potential to drive innovations in sustainable energy management and optimization methodologies.

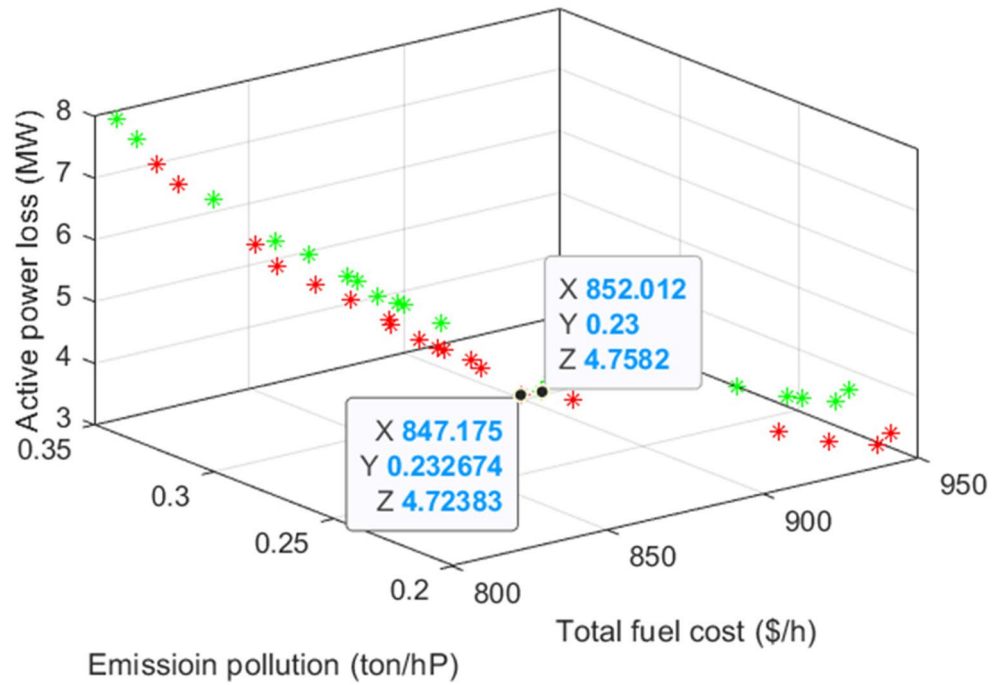


Figure 4. Pareto front obtained in Case 3.

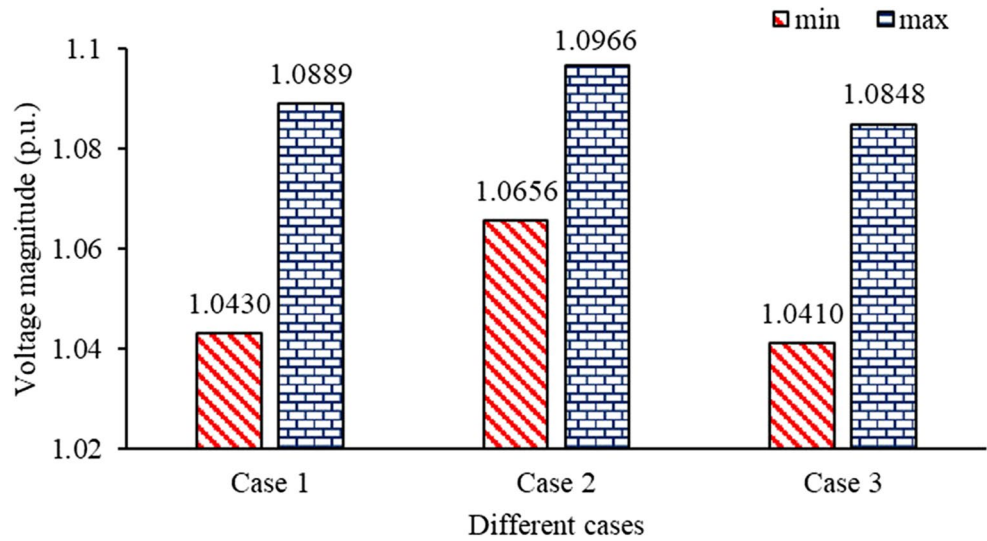


Figure 5. Minimum and maximum load bus voltages obtained in all cases.

Data availability

The datasets generated during and/or analysed during the current study are available from the corresponding author on reasonable request.

Received: 7 July 2024; Accepted: 21 October 2024

Published online: 04 November 2024

References

1. Dommel, H. W. & Tinney, W. F. Optimal power flow solutions. *IEEE Trans Power Appar Syst.* **87**, 1866–1876 (1968).
2. Scott, B. & Hobson, E. Power system security control calculations using linear programming- part I. *IEEE Trans. Power Appar Syst.* **97** (5), 1713–1720 (1978).
3. Sun, D. I., Ashley, B., Brewer, B. & Tinney, W. F. Optimal powerflow by Newton approach. *IEEE Trans Power Appar Syst.* **103** (10), 2864–2880 (1984).

4. Omar, A. A., AL-Smadi, M., Shaher, M. & Tasawar, H. Numerical solutions of fuzzy differential equations using reproducing kernel Hilbert space method. *Soft Comput.* **20** (8), 3283–3302 (2016).
5. Omar, A. A., AL-Smadi, M., Shaher, M. & Tasawar, H. Application of reproducing kernel algorithm for solving second-order, two-point fuzzy boundary value problems. *Soft. Comput.* **21** (13), 7191–7206 (2017).
6. Omar, A. A. Adaptation of reproducing kernel algorithm for solving fuzzy Fredholm-Volterra integrodifferential equations. *Neural Comput. Appl.* **28** (7), 1591–1610 (2017).
7. Pulluri, H., Sharma, R. N. & Sharma, V. An enhanced self-adaptive differential evolution based solution methodology for multiobjective optimal power flow. *Appl. Soft Comput.* **54**, 229–245 (2017).
8. Surender Reddy, S. & Bijwe, P. R. Differential evolution-based efficient multi-objective optimal power flow. *Neural Comput. Applic.* **31**, 509–522 (2019).
9. Abido, M. A. Al-Ali. Multiobjective optimal power flow using differential evolution. *Arab. J. Sci. Eng.* **37**, 991–1005 (2012).
10. uman, S., Akbel, M. & Kahraman, H. T. Development of the multi-objective adaptive guided differential evolution and optimization of the MO-ACOPF for wind/PV/tidal energy sources. *Appl. Soft Comput.* **112**, 107814 (2021).
11. Deb, K., Agarwal, S., Pratap, A. & Merayivan, T. A fast and elitist multiobjective genetic algorithm: NSGA-II. *IEEE Trans. Evol. Comput.* **6** (2), 182–197 (2002).
12. Ragab, A. E., Selim, F., Bachir, B. & bido, M. A. A novel multi-objective hybrid particle swarm and salp optimization algorithm for technical-economic environmental operation in power systems. *Energy.* **193**, 116817 (2020).
13. Rezaei, M., Daryani, A. & Karami, M. Artificial bee colony algorithm for solving multiobjective optimal power flow problem. *Int. J. Electr. Power Energy Syst.* **53**, 219–230 (2013).
14. Sivasubramani, S. & Swarup, K. S. Multiobjective harmony search algorithm for optimal power flow problem. *Int. J. Electr. Power Energy Syst.* **33**, 745–752 (2011).
15. Aniruddha, B. & Provas, K. R. Solution of multi-objective optimal power flow using gravitational search algorithm. *IET Gener. Transm. Distr.* **6** (8), 751–763 (2012).
16. Arup, R. B. & Ajoy, K. C. Solution of optimal power flow using non dominated sorting multi objective opposition based gravitational search algorithm. *Int. J. Electr. Power Energy Syst.* **64**, 1237–1250 (2015).
17. Li, N. *et al.* Multi-objective pathfinder algorithm for multi-objective optimal power flow problem with random renewable energy sources: wind, photovoltaic and tidal. *Sci. Rep.* **13**, 10647 (2023).
18. Ghasemi, M., Ghavidel, S., Ghanbarian, M. M. & Gitzadeh, M. Multiobjective optimal electric power planning in the power system using Gaussian bare-bones imperialist competitive algorithm. *Inf. Sci.* **294**, 286–304 (2015).
19. Chen, M. R., Yang, L. Q. & Zeng, G. Q. IFA-EO: an improved firefly algorithm hybridized with extremal optimization for continuous unconstrained optimization problems. *Soft Comput.* **27** (6), 2943–2964 (2023).
20. Li, H., Wang, Z., Zeng, N., Wu, P. & Li, Y. Promoting objective knowledge transfer: a cascaded fuzzy system for solving dynamic Multiobjective optimization problems. in *IEEE Trans. Fuzzy Syst.*, <https://doi.org/10.1109/TFUZZ.2024.3443207>
21. Li, H., Wang, Z., Lan, C., Wu, P. & Zeng, N. A novel dynamic multiobjective optimization algorithm with non-inductive transfer learning based on multi-strategy adaptive selection. *IEEE Trans. Neural Netw. Learn. Syst.* **28** <https://doi.org/10.1109/TNNLS.2023.3295461> (2023).
22. Naderi, E., Mirzaei, L., Trimble, J. P. & Cantrell, D. A. multi-objective optimal power flow incorporating flexible alternating current transmission systems: application of a wavelet-oriented evolutionary algorithm. *Electr. Power Compo Syst.* **52** (5), 766–795 (2023).
23. Li, H., Wang, Z., Lan, C., Wu, P. & Zeng, N. A novel dynamic multiobjective optimization algorithm with hierarchical response system. *IEEE Trans. Comput. Social Syst.* **11** (2), 2494–2512 (2024).
24. Pulluri, H., Naresh, R. & Sharma, V. A solution network based on stud krill herd algorithm for optimal power flow problems. *Soft Comput.* **22** (1), 159–176 (2016).
25. Beibei, S. *et al.* Prediction of recurrent spontaneous abortion using evolutionary machine learning with joint self-adaptive sine mould algorithm. *Comput. Biol. Med.* **148**, 105885 (2022).
26. Kaveh, A. & Mahdvi, V. R. Colliding bodies optimization: a novel meta-heuristic method. *Comput. Struct.* **139**, 8–27 (2014).
27. Pulluri, H., Naresh, R., Sharma, V. & Preeti Solving non-convex and non-linear optimal power flow problems using colliding bodies optimization, Proceedings of the 2nd international Conference on Recent Advances in Engineering and Computer Sciences (RAECS-2015), Chandigarh, INDIA, pp. 1–6. (2015).
28. Pulluri, H., Naresh, R., Sharma, V. & Preeti A new colliding bodies optimization for solving optimal power flow problem in power system. Proceedings of the 6th International Conference on Power Systems (ICPS – 2016), New Delhi, INDIA, pp. 1–6. (2016).
29. Kaveh, A. & Mahdvi, V. R. Colliding bodies optimization method for optimum design of truss structures with continuous variables. *Adv. Eng. Soft.* **70**, 1–12 (2014).
30. Gouthamkumar, N., Srinivasarao, B., Venkateswararao, B. & Narasimham, P. V. R.L. Nondominated sorting-based disruption in oppositional gravitational search algorithm for stochastic multiobjective short-term hydrothermal scheduling. *Soft Comput.* **23** (16), 7229–7248 (2019).

Author contributions

All authors have contributed equally. All authors reviewed the manuscript.

Funding

The authors declare that no funds, grants or other support were received during the preparation of this manuscript.

Declarations

Ethical approval

The paper is not currently being considered for publication elsewhere.

Consent to participate

Not applicable.

Consent to publish

Not applicable.

Competing interests

The authors declare no competing interests.

Additional information

Correspondence and requests for materials should be addressed to S.K.

Reprints and permissions information is available at www.nature.com/reprints.

Publisher's note Springer Nature remains neutral with regard to jurisdictional claims in published maps and institutional affiliations.

Open Access This article is licensed under a Creative Commons Attribution-NonCommercial-NoDerivatives 4.0 International License, which permits any non-commercial use, sharing, distribution and reproduction in any medium or format, as long as you give appropriate credit to the original author(s) and the source, provide a link to the Creative Commons licence, and indicate if you modified the licensed material. You do not have permission under this licence to share adapted material derived from this article or parts of it. The images or other third party material in this article are included in the article's Creative Commons licence, unless indicated otherwise in a credit line to the material. If material is not included in the article's Creative Commons licence and your intended use is not permitted by statutory regulation or exceeds the permitted use, you will need to obtain permission directly from the copyright holder. To view a copy of this licence, visit <http://creativecommons.org/licenses/by-nc-nd/4.0/>.

© The Author(s) 2024